Phonon Self-Energy Corrections to Nonzero Wave-Vector Phonon Modes in Single-Layer Graphene

P. T. Araujo, D. L. Mafra, K. Sato, R. Saito, J. Kong, and M. S. Dresselhaus

Phys. Rev. Lett. **109**, 046801 — Published 24 July 2012

DOI: 10.1103/PhysRevLett.109.046801

Phonon self-energy corrections to non-zero wavevector phonon modes in single-layer graphene

P. T. Araujo[1,†], D. L. Mafra[1,2,†], K. Sato[3], R. Saito[3], J. Kong[1] and M. S. Dresselhaus[1,4]
[1] *Department of Electrical Engineering and Computer Sciences, Massachusetts Institute of Technology, Cambridge, MA 02139-4307, USA.*
[2] *Departamento de Física, Universidade Federal de Minas Gerais, Belo Horizonte, MG, 30123-970 Brazil.*
[3] *Department of Physics, Tohoku University, Sendai 980-8578, Japan.*
[4] *Department of Physics, Massachusetts Institute of Technology, Cambridge, MA 02139-4307, USA.*
[†] *These authors contributed equally to this work.*
(Dated: June 18, 2012.)

Phonon self-energy corrections have mostly been studied theoretically and experimentally for phonon modes with zone-center ($q = 0$) wave-vectors. Here, gate-modulated Raman scattering is used to study phonons of a single layer of graphene (1LG) originating from a double-resonant Raman process with $q \neq 0$. The observed phonon renormalization effects are different from what is observed for the zone-center $q = 0$ case. To explain our experimental findings, we explored the phonon self-energy for the phonons with non-zero wave-vectors ($q \neq 0$) in 1LG in which the frequencies and decay widths are expected to behave oppositely to the behavior observed in the corresponding zone-center $q = 0$ processes. Within this framework, we resolve the identification of the phonon modes contributing to the G* Raman feature at 2450 cm^{-1} to include the iTO+LA combination modes with $q \neq 0$ and also the 2iTO overtone modes with $q = 0$, showing both to be associated with wave-vectors near the high symmetry point **K** in the Brillouin zone.

PACS numbers: 73.20.Hb, 73.22.-f, 78.30.Na, 78.67.Ch

Electron-phonon (el-ph) interactions are responsible for many important effects in condensed matter physics [1]. In particular, the phonon self-energy, which is mainly due to the el-ph coupling, is a remarkable effect which contributes to both the phonon frequency and decay width renormalizations due to the creation (annihilation) of electron-hole (e-h) pairs through phonon absorption (emission). These phonon self-energy corrections are needed to explain a set of well-known effects, such as the Kohn anomaly [1, 2], the Peierls transition [1, 3, 4], polaron formation [1, 5, 6], and other types of phonon renormalizations and perturbations [7–10].

Particularly special, single-layer graphene (1LG) has linear electronic energy dispersions $E(k)$ around the non-equivalent high symmetry points **K** and **K′** in the Brillouin zone as a solution of the Dirac equation which gives massless particle behavior around **K** (**K′**) [11]. However, one cannot properly solve the electronic and vibrational structure for most nanocarbon materials near the Dirac points when considering the adiabatic approximation, which disregards the ionic motion of the carbon ions [12–14]. When the adiabatic approximation cannot be applied [1, 2], el-ph interactions are needed to take into account non-adiabatic processes, which give rise to important and strong phonon self-energy corrections [1]. Within second-order perturbation theory, the phonon self-energy can be approximately described as [1, 2, 9, 10]:

$$\Pi(\omega_{\mathbf{q}}, E_F) = 2\sum_{\mathbf{kk'}} \frac{|\mathrm{V}_{\mathbf{kk'}}|^2}{\hbar\omega_{\mathbf{q}} - E^{eh} + i\gamma_{\mathbf{q}}/2} \times (f_h - f_e) \quad (1)$$

where **k** and **k′** are, respectively, wave-vectors for the initial and final electronic states; $\mathbf{q} \equiv \mathbf{k} - \mathbf{k'}$ is the phonon wave-vector; $E^{eh} \equiv (E^e_{\mathbf{k'}} - E^h_{\mathbf{k}})$ is the e-h pair energy; $\omega_{\mathbf{q}}$ is the phonon frequency; $\gamma_{\mathbf{q}}$ is the phonon decay width; $f_h(f_e)$ is the Fermi distribution function for holes (electrons) and $\mathrm{V}_{\mathbf{kk'}}$ gives the el-ph coupling matrix element. For a specific $\omega_{\mathbf{q}}$, the phonon energy correction due to its self-energy is given by $\hbar\omega_{\mathbf{q}} - \hbar\omega^0_{\mathbf{q}} = \mathrm{Re}[\Pi(\omega_{\mathbf{q}}, E_F)]$, which is the real part of Eq.1, where $\hbar\omega^0_{\mathbf{q}}$ is the phonon energy in the adiabatic approximation. Likewise, the decay width $\gamma_{\mathbf{q}}$ is given by the imaginary part of $\mathrm{Im}[\Pi(\omega_{\mathbf{q}}, E_F)]$ of Eq. 1 [1, 2, 9].

These phonon renormalizations occur any time we have non-zero matrix elements $\mathrm{V}_{\mathbf{kk'}}$ and occupied (unoccupied) initial (final) states, in the sense that an electron-hole pair can be created (annihilated) by a phonon absorption (emission) process as a perturbation. In Eq. 1, although the summation is performed over all the electronic states, the combination of electronic states that fulfills the momentum and energy requirements for a given phonon will be the ones to significantly contribute to the phonon self-energy. In other words, this combination of states will present a non-null $\mathrm{V}_{\mathbf{kk'}}$ and a resonant behavior given by the denominator of Eq. 1. There are two types of electron-phonon interactions, namely intra-valley (AV) (Figs. 1(a) and 2(b)) and inter-valley (EV) (Figs. 2(a) and (c)) processes [15]. For an AV process, the initial and final states both occur within the region close to a **K** [**K′**] point, while for inter-valley processes, **K** is connected to **K′** (or **K′** to **K**), respectively, in a different valley by a $q \neq 0$ phonon. Thus the AV (EV) process corresponds to **Γ** (**K**) point phonons. The phonon wavevector **q** for AV (EV) processes are measured from

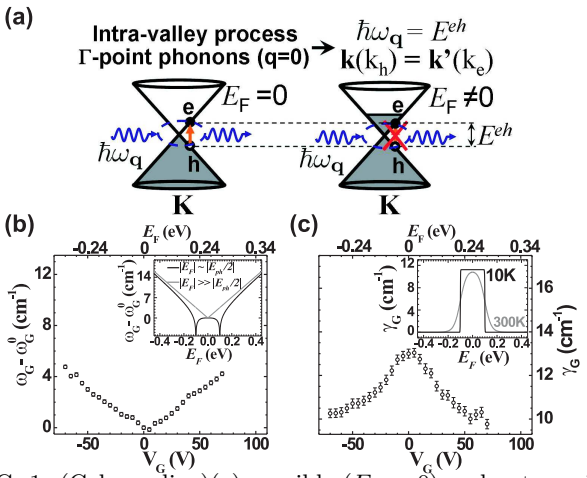

FIG. 1: (Color online)(a) possible ($E_F = 0$) and not possible ($E_F \neq 0$) AV $q = 0$ processes for e-h pair creation (annihilation) due to phonon (with energy $\hbar\omega_{\mathbf{q}}$) absorption (emission). E^{eh} stands for the e-h pair energy. (b) and (c) show, respectively, the frequency ω_G hardening and decay width γ_G narrowing for the G-band Raman feature as a function of gate voltage V_G. The insets in (b) and (c) are theoretical predictions based on Ref. [2] of the E_F dependence of $\hbar\omega_{\mathbf{q}} - \hbar\omega_{\mathbf{q}}^0$ and $\gamma_{\mathbf{q}}$ for an AV $q = 0$ process. The E_F values on the upper scales are obtained with $E_F = \hbar|v_F|\sqrt{\pi C_g V_G/e}$, where $C_g = 115aF/\mu m^2$ is the gate capacitance per unit of area, e is the electron charge and $|v_F| = 1.1\times10^6$ m/s is the carrier Fermi velocity.

the $\mathbf{\Gamma}$ ($\mathbf{K}$) points with both $q = 0$ and $q \neq 0$ possible.

Previously, most discussions of phonon self-energy renormalizations have been for zone-center phonons ($\mathbf{\Gamma}$-point) with $q = 0$, which can be appreciated by observing the G-band Raman feature evolution in 1LG as the Fermi energy (E_F) is varied (see Figs. 1(b) and (c))[7, 10, 16–18]. In the present work, we use gate-modulated resonant Raman spectroscopy (RRS) to address the effect of a E_F variation due to applying a gate voltage (V_G) to the phonon self-energy (Eq.1), for 1LG systems, in cases where $q \neq 0$ (AV and EV processes). These cases have not been sufficiently studied previously. Here, we study the double resonance Raman frequency ranges between 2350 and 2850 cm^{-1}, which contain the G* and the G$'$-band spectral features as shown in Fig. 3(a) [11, 19, 20]. We show below that the phonon renormalization for $q \neq 0$ phonons ($\mathbf{K}$-point phonons) gives an E_F dependence different from that for $q = 0$ $\mathbf{\Gamma}$-point phonons. We show that these differences in behavior can be used to observe that the G* feature is composed of two Raman peaks which behave differently from one another as $|V_G|$ is varied.

The graphene flakes used in our experiments were obtained by micro-mechanical exfoliation of graphite over Si substrates with a 300 nm thick layer of SiO_2. Next, e-beam lithography was performed to pattern our devices. Then, thermal evaporation of Cr/Au (5 and 80 nm, respectively) was done. For each V_G value, RRS spectra were taken with a 532 nm wavelength laser source in the backscattering geometry using a 100X objective. The laser power measured from the objective was 1.5 mW. The spectra were analyzed using Lorentzian line-shapes from which frequencies and decay widths were extracted [21]. Figures 1(b) and (c) and Figs. 3(a)-(e) show the experimental results [22]. Note that RRS provides information about both the electronic and vibrational structures, while the V_G variation allows for control of E_F. We show that, due to the difference in behavior between the $q = 0$ and $q \neq 0$ processes, this combination of techniques provides a precise way to verify the assignments of either overtones and/or a combination of phonon modes.

The G* and G$'$ features were intentionally chosen for this discussion because: (1) they are the most prominent double-resonance Raman features in the graphene spectrum, offering a convenient platform, together with the G-band feature, to observe experimentally the two different types of phonon renormalizations, one found for the $q = 0$ phonons and the other for $q \neq 0$ phonons, and (2) as a consequence of these different phonon renormalization effects, we have solved a long-time discussion in the literature, showing that the G* feature is composed of both the iTO+LA ($q = 2k$) and 2iTO ($q = 0$) Raman active modes, both measured from the $\mathbf{K}$-point. In the literature, the G* feature around 2450 cm^{-1} has been assigned to either the iTO+LA phonon combination mode ($q = 2k$ EV process) [20], or to the 2iTO phonon overtone mode ($q = 0$ EV process) [19], awaiting a more definitive assignment. Note the possibility of two types of double resonance conditions, $q = 0$ and $q = 2k$, for a phonon with momentum $\mathbf{q}$ and an electron with momentum $\mathbf{k}$ [23, 24]. The G$'$ (or 2D) feature at 2670 cm^{-1} is widely known to be an overtone of the iTO phonon mode ($q = 2k$) [11, 19, 20]. It gives a dispersive phonon frequency as a function of laser energy $E_{\rm Laser}$ which exhibits the value of 103 cm^{-1}/eV [25]. The iTO+LA ($q = 2k$) combination mode presents a dispersion of -(16±1) cm^{-1}/eV (measured in this work), while the 2iTO ($q = 0$) overtone mode (also measured in this work) is not dispersive (see Fig. 3(b)). Figure 3(a) shows that indeed the G* feature is asymmetric, suggesting that it consists of two Lorentzians peaks rather than just one.

Equation 1 has previously been explored for the cases where the phonon momentum $\mathbf{q}$ vanishes ($q = 0$) for the AV intra-valley process. In these cases, at zero temperatures (T=0), the phonon energy correction $\hbar\omega_{\mathbf{q}} - \hbar\omega_{\mathbf{q}}^0$ is:

$$\hbar\omega_{\mathbf{q}} - \hbar\omega_{\mathbf{q}}^0 = \alpha|E_F| + \frac{\alpha\hbar\omega_{\mathbf{q}}^0}{4} ln\left(\left|\frac{2|E_F| - \hbar\omega_{\mathbf{q}}^0}{2|E_F| + \hbar\omega_{\mathbf{q}}^0}\right|\right) \quad (2)$$

where $\alpha/(2c\pi\hbar) = 35.8$ cm^{-1} [2], while $\gamma_{\mathbf{q}}$, which will be proportional to the el-ph coupling strength, gives the damping of the phonon mode due to real e-h pair creation (annihilation) [2, 9, 17, 18]. The insets of Figs. 1(b)

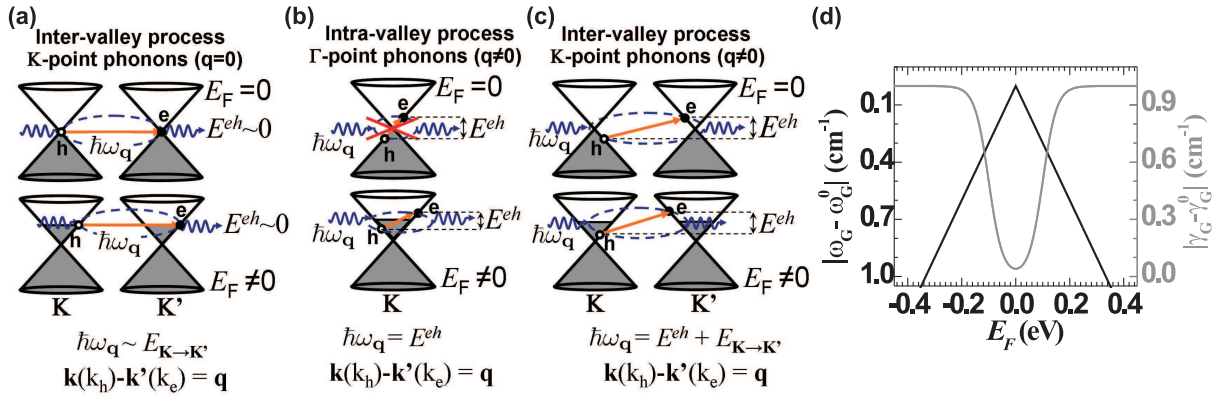

FIG. 2: (Color online) (a) possible ($E_F = 0$ and $E_F \neq 0$) $q = 0$ (measured from the **K** point) EV processes, (b) not possible ($E_F = 0$) and possible ($E_F \neq 0$) AV processes and (c) possible EV processes for electron-hole pair creation (annihilation) due to phonon (with energy $\hbar\omega_{\mathbf{q}}$) absorption (emission) when the phonon wave-vector is not zero ($q \neq 0$). (d) shows illustrative predictions for the V_G-dependence of the phonon frequency correction $\omega_{\mathbf{q}} - \omega_{\mathbf{q}}^0$ (black solid line) and the corresponding decay width $\gamma_{\mathbf{q}}$ (grey dashed line) when $q \neq 0$, both as a function of E_F. The $\omega_{\mathbf{q}} - \omega_{\mathbf{q}}^0$ and $\gamma_{\mathbf{q}}$ values in (d) were normalized to illustrate the concept of $\omega_{\mathbf{q}}$ softening and $\gamma_{\mathbf{q}}$ broadening. E^{eh} is the e-h pair energy and $E_{\mathbf{K}\to\mathbf{K}'}$ is the energy required to translate an electron from **K** to **K**′ [26].

and (c), which were based on Ref. [2], give the results illustrated for the renormalization of $\omega_{\mathbf{q}}$ and $\gamma_{\mathbf{q}}$, respectively. From these insets and Eq.2, we observe that when $2|E_F| < \hbar\omega_{\mathbf{q}}$, real e-h pairs can be created (annihilated), which leads to a stronger electron-ion interaction screening. As a consequence, the phonon mode softens [2, 9, 17, 18]. However, when $2|E_F| > \hbar\omega_{\mathbf{q}}$ the production of real e-h pairs becomes forbidden due to the Pauli principle. This leads to a phonon mode hardening where the phonons are not damped any more (they are now long lived) [2, 9, 17, 18]. But what happens if $2|E_F| = \hbar\omega_{\mathbf{q}}$? In this situation, the phonon mode softening shows its highest values, which represent two singularities in Eqs. 1 and 2, as shown by the black solid curve in the inset of Fig. 1(b). These singularities give rise to what is commonly known as Kohn-anomalies. As an example of phonon renormalization when $q = 0$ for the AV process (see Fig. 1(a)), the ω_G and γ_G variations of the G-band Raman feature are shown in Figs. 1(b) and (c), respectively, as $|E_F|$ is varied due to different V_G values. The experimental results (Figs. 1(b) and (c)) are in good agreement with theory [2, 16–18], which shows a ω_G hardening and γ_G narrowing when V_G increases. Note that the absence of Kohn-anomalies is expected because of a broadening (comparable to the phonon energy) in $|E_F|$ due to thermal excitations (relaxations) and non-uniformity in the density of carriers (due to foreign chemical species and charge traps in the substrate)[17, 18]. Next, we report the new experimental results for phonons corresponding to the cases $q = 0$ EV (inter-valley) and $q \neq 0$ AV/EV processes.

Both the G* iTO+LA mode at 2450-53 cm^{-1} and the G′ mode at 2670-73 cm^{-1} are EV double-resonance Raman processes with $q \neq 0$ (see Fig. 3(a)) and, as shown in Figs. 3(c)-(e), they both show a different behavior when V_G increases compared to the behavior observed for the AV $q = 0$ process. Starting with the G′-band feature (the 2iTO $q = 2k$ EV process around the **K**-point), it is seen that its frequency $\omega_{G'}$ decreases with increasing $|V_G|$ (Fig. 3(c)), while its decay width $\gamma_{G'}$ increases with increasing $|V_G|$ (see the inset in Fig. 3(c)). Here, we see that the same behavior is observed for the iTO+LA mode frequency $\omega_{\mathrm{iTO+LA}}$ ($q = 2k$ EV process around the **K**-point), as shown in Fig. 3(d), and for its decay width $\gamma_{\mathrm{iTO+LA}}$, as shown in Fig. 3(e). The 2iTO G* feature at 2470-73 cm^{-1}, which is a $q = 0$ EV process around the **K** point (see Fig. 2(a)), is observed in Figs. 3(d) and (e) to show a frequency ω_{2iTO} and a decay width γ_{2iTO} that almost do not change with increasing $|V_G|$. This behavior shows that the 2iTO ($q = 0$) mode couples only weakly to the electronic states in graphene and therefore its phonon self-energy corrections are small.

To explain our experimental findings, a phenomenological formulation for the phonon self-energy for the EV $q = 0$ and AV/EV $q \neq 0$ processes in single-layer graphene are presented. But first, the reader should review what happens for phonons with $q = 0$: in the case of AV processes for the $q = 0$ phonons, which applies to the G-band feature (see Fig. 1), the creation (annihilation) of a real e-h pair is very high when $E_F = 0$, which implies a phonon frequency ($\omega_{\mathbf{q}}$) softening and phonon decay width (γ) broadening. With increasing $|E_F|$, $\omega_{\mathbf{q}}$ hardens and $\gamma_{\mathbf{q}}$ narrows, which means that the real e-h pair creation (annihilation) is being halted by the Pauli principle because the phonon energy is becoming smaller than $2|E_F|$. Next, we see that this approach can now be used to understand the EV $q = 0$ and AV/EV $q \neq 0$ processes considering a small difference: now, instead of the Pauli principle, the density of phonon and electronic states, as well as the energy and momentum conservation

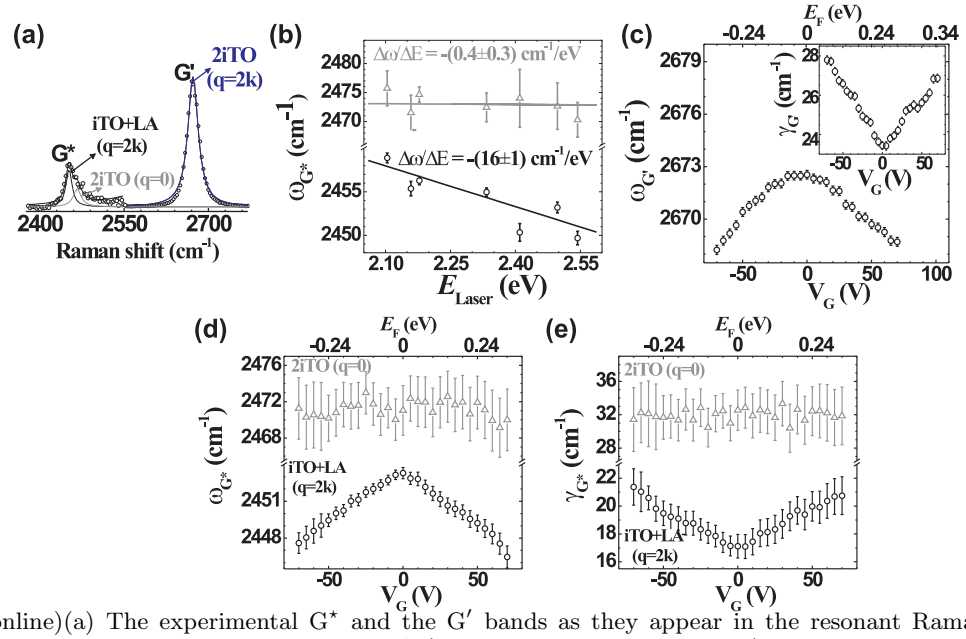

FIG. 3: (Color online)(a) The experimental G* and the G$'$ bands as they appear in the resonant Raman spectrum. The asymmetric G* feature is a combination of the iTO+LA ($q = 2k$ read from the **K** point) mode and the 2iTO ($q = 0$ read from the **K** point) mode. The G$'$ mode is an overtone of the iTO mode ($q = 2k$). For illustrative purposes, the signal of the G* feature was multiplied by a factor of 10 and the Lorentzian profiles used to fit the spectrum are shown in constructing (a). (b) The frequency dispersion of the G* peaks as a function of laser energy ($E_{\rm Laser}$) and shows that the iTO+LA ($q = 2k$) is a dispersive mode, while the 2iTO ($q = 0$) is non-dispersive [19, 20]. (c) The gate voltage V_G dependence of the 2iTO ($q = 2k$) $\omega_{\mathbf{G}'}$ and $\gamma_{\mathbf{G}'}$ (inset in (c)). (d) and (e) show, respectively, the $\omega_{\mathbf{q}}$ and $\gamma_{\mathbf{q}}$ dependencies on $|E_{\rm F}|$ seen for the iTO+LA and 2iTO modes. In (c), (d) and (e), the E_F values were calculated as explained in the caption of Fig. 1.

requirements, will be responsible for halting the real e-h pair creation (annihilation).

As shown above, a different behavior is expected for the $q = 0$ phonon (measured from **K**-point) in the EV process shown in Fig. 2(a), which explains the G* 2iTO mode behavior as $|E_{\rm F}|$ is varied with varying V_G. According to the Fermi golden-rule, the probability that a real electron-hole pair exists at $E_{\rm F} = 0$ (upper line of Fig. 2) is quite small since the density of states of both, electrons and phonons, at $E_{\rm F}$ almost vanishes [10, 11]. Therefore, no softening of $\omega_{\mathbf{q}}$ and no broadening of $\gamma_{\mathbf{q}}$ is expected, since almost no real electron-hole pair is being created (annihilated). When $|E_{\rm F}|$ increases (lower line in Fig. 2), the probability for a **K**-point $q = 0$ phonon to connect inequivalent energy $\mathbf{k}$ and $\mathbf{k}'$ states ($k = k'$) increases, because the density of phonon and electron states also increases as we move away from the **K**-point [10, 11]. This means that the number of real e-h pair creations (annihilations) increases and thus the phonon mode softening and damping effects could be observed with increasing $|E_{\rm F}|$. However, for EV processes, part of the phonon energy is used to translate the electron from **K** to **K**$'$ (which requires an energy $E_{\mathbf{K}\rightarrow\mathbf{K}'}$ charged to the system) and, therefore, the remaining phonon energy to create an e-h pair is small so that $E^{eh} \sim 0$, where E^{eh} is the e-h pair energy. This means that $\omega_{\mathbf{q}} - \omega^0_{\mathbf{q}}$ will be a small correction and, therefore, small $\omega_{\mathbf{q}}$ softenings and small $\gamma_{\mathbf{q}}$ dampings are expected for any $|E_{\rm F}|$ value (weak $E_{\rm F}$-dependence).

By considering phonon modes with $q \neq 0$ (AV and EV processes) as shown in Figs. 2(b) and (c), the phonon wave-vectors are either around the $\mathbf{\Gamma}$ point or around the **K** point. These cases explain the G$'$ and the G* iTO+LA mode behaviors as $|V_G|$ is varied. Since the phonon and electron density of states are small close to the **K**(**K**$'$) points and since the phonon energy dispersion for graphene has a much smaller slope than that for the electronic energy dispersions [11], there is essentially no coupling between $q \neq 0$ phonons and e-h pairs (there is no $\mathbf{q}$ such that $\mathbf{q} = \mathbf{k} - \mathbf{k}'$) if $E_{\rm F} = 0$ and therefore the softening and damping of the phonon mode in this case does not take place in a resonant way, *i.e.* where $E^{eh} = \hbar\omega_{\mathbf{q}}$ for the AV process and $E_{\mathbf{K}\rightarrow\mathbf{K}'} + E^{eh} = \hbar\omega_{\mathbf{q}}$ for the EV process. If no phonons with $q \neq 0$ can connect electronic states with different $\mathbf{k}$ and $\mathbf{k}'$ at $E_{\rm F} = 0$, the matrix elements $V_{\mathbf{k}\mathbf{k}'}$ in Eq. 1 are close to zero and essentially no self-energy corrections occur. Precisely speaking, in the case of the EV process (Fig. 2(c)), the e-h pair creation (annihilation) is possible for $E_{\rm F} = 0$ but, as stated above, the density of phonon and electron states is very small at $E_{\rm F} \sim 0$ which makes the probability for the e-h pair creation (annihilation) also small. However, when $E_{\rm F} \neq 0$, the density of phonon and electron states increases and phonon modes with $q \neq 0$ can now connect electronic states with different $\mathbf{k}$ and $\mathbf{k}'$, in the sense that there is a $\mathbf{q}$ such that $\mathbf{q} = \mathbf{k} - \mathbf{k}'$ (the differences

between slopes in the electron and phonon dispersion decrease when we move away from the **K**-point [11]). This gives rise to a strong electron-phonon coupling which enhances the creation(annihilation) of real e-h pairs. As a consequence, the phonon mode softens ($\omega_{\mathbf{q}}$ decreases) and gets damped ($\gamma_{\mathbf{q}}$ broadens) as shown in Figs. 2(b) and (c). This $q \neq 0$ (AV and EV processes) behavior is illustrated in Fig. 2(d), where it is seen that the frequency softening (black solid line) must increase with increasing $|E_{\rm F}|$ while the decay width (grey solid line) must broaden with increasing $|E_{\rm F}|$.

In summary, the widely studied intra-valley AV $q = 0$ case [2, 16–18] shows that when $E_{\rm F} = 0$ the phonon softening and damping is maximum due to real e-h pair creation (annihilation) and decrease with increasing $|E_{\rm F}|$. Here, we have shown that in the $q \neq 0$ cases (oppositely to what is observed for the $q = 0$ AV process), the phonon softening and damping is a minimum when $E_{\rm F} = 0$ and increases with increasing $|E_{\rm F}|$. For the EV $q = 0$ case, $E^{eh} \sim 0$ and a weak and small $\omega_{\mathbf{q}}$ and $\gamma_{\mathbf{q}}$ dependence with $E_{\rm F}$ is expected. Due to these different phonon self-energy behaviors, gate-modulated resonant Raman spectroscopy provides a powerful technique to assign the phonons participating in the formation of overtones or combination modes, to identify whether a Raman feature is associated with the $q = 0$ or the $q \neq 0$ processes and to determine how a given phonon mode is coupled to the electronic states of single-layer graphene. As shown in Figs. 3(a)-(e), we applied these combined techniques to study the G* and G$'$ modes, which are the most prominent double resonance $q \neq 0$ Raman features in the SLG graphene spectrum. Within this framework, we also showed that the G* mode is an asymmetric peak composed by both, the iTO+LA combination mode, which is an EV $q = 2k$ process with a strong phonon renormalization, and the 2iTO overtone mode, which is an EV $q = 0$ process with a weak phonon renormalization, thereby resolving a long-time discussion in the literature. Finally, the principles applied to this frequency range can be applied to any other features in the RRS.

Acknowledgments

P.T.A. and D.L.M. acknowledge CNPq and NSF-DMR 10-04147 grants. R.S. and K.S. acknowledge MEXT grant (No.20241023). M.S.D acknowledges NSF-DMR 10-04147. J.K. acknowledges NSF-DMR 08-45358.

[1] P. L. Taylor and O. Heinonen, *A quantum approach to condensed matter physics*. (University Press Cambridge, United Kingdom, 2004).

[2] M. Lazzeri and F. Mauri, *Phys. Rev. Lett.* **97**, 266407 (2006).

[3] O. Dubay, G. Kresse, and H. Kuzmany, *Phys. Rev. Lett.* **88**, 235506 (2002).

[4] A. Sedeki, L. G. Caron, and C. Bourbonnais, *Phys. Rev.* B **62**, 6975 (2000).

[5] V. M. Stojanovic, N. Vukmirovic and C. Bruder, *Phys. Rev.* B **82**, 165410 (2010).

[6] C. Nisoli, *Phys. Rev.* B **80**, 113406 (2009).

[7] H. Farhat *et al.*, *Phys. Rev. Lett.* **102**, 126804 (2009).

[8] C. H. Park *et al.*, *Nano lett.* **8**, 4229 (2008).

[9] K. Sasaki *et al.*, *Physica E* **42**, 2005 (2010).

[10] A. H. Castro Neto *et al.*, *Rev. Mod. Phys.* **81**, 109 (2009).

[11] A. Jorio, M. S. Dresselhaus, R. Saito and G. Dresselhaus, *Raman Spectroscopy in Graphene Related Systems.* (WILEY-VCH, Weinheim, 2011).

[12] K. S. Novoselov *et al.*, *Nature* **438**, 197 (2005).

[13] J. C. Meyer *et al.*, *Nature* **446**, 60 (2007).

[14] S. Pisana *et al.*, *Nat. Materials* **6**, 198 (2007).

[15] J. Jiang *et al.*, *Carbon* **392**, 383 (2004).

[16] L. M. Malard, D. C. Elias, E. S. Alves, and M. A. Pimenta, *Phys. Rev. Lett.* **101**, 257401 (2008).

[17] J. Yan, E. A. Henriksen, P. Kim, and A. Pinczuk, *Phys. Rev. Lett.* **101**, 136804 (2008).

[18] J. Yan *et al.*, *Solid State Comm.* **143**, 39 (2007).

[19] T. Shimada *et al.*, *Carbon* **43**, 1049 (2005).

[20] D. L. Mafra *et al.*, *Phys. Rev.* B **76**, 233407 (2007).

[21] It is important to comment that the Raman spectral lineshapes have a certain width, which gives us an uncertainty in the observed phonon energy. Since Eqs. 1 and 2 depend on both, $\omega_{\mathbf{q}}$ and $E_{\rm F}$, for each $E_{\rm F}$ the self energy corrections could give rise to a departure from the traditional Lorentzian line-shape (used to fit the spectra) due to different phonon self-energy corrections for different $\omega_{\mathbf{q}}$ along the spectral line width. By using Eqs. 1 and 2, we see that the self-energy correction variations $[\Delta(\omega_{\mathbf{q}} - \omega^0_{\mathbf{q}})/\Delta\omega_{\mathbf{q}}$ and $\Delta\gamma_{\mathbf{q}}/\Delta\omega_{\mathbf{q}}]$ due to different $\omega_{\mathbf{q}}$ along the spectral width, for each $E_{\rm F}$ applied, are of order of 10^{-4}! This variation is very small to cause a spectral line-shape departure from a Lorentzian line-shape. Indeed, the experiment shows that the Lorentizian lineshapes are suitable to fit the spectra.

[22] The Si/SiO_2 interface produces bulk traps whose charge states change continuously with $V_{\rm G}$. These traps give rise to hysteresis effects, and nominal changes in the Dirac point position $\Delta V_{\rm DP} = (8 - 20)$ V are expected. The $\Delta V_{\rm DP}$ generates a charge density variation $\Delta n = (0.03 - 0.07) \times 10^{13}$ cm^{-1} that, according to Ref.[2], represents an uncertainty of less than 2 cm^{-1} in $\omega_{\mathbf{q}}$. The phonon energies in this work correspond to $\Delta n = (0.09 - 0.23) \times 10^{13}$ cm^{-1}. Therefore, the charge traps could prevent observation of Kohn-anomalies but not the general behavior of self-energy corrections, as observed in this work.

[23] R. Saito *et al.*, *Phys. Rev. Lett.* **88**, 027401 (2001).

[24] R. Saito *et al.*, *New J. Phys.* **5**, 157 (2003).

[25] A. G. Souza Filho *et al.*, *Phys. Rev.* B **65**, 035404 (2001).

[26] Remember that the energy is not conserved when going from **K** to **K**$'$. They are inequivalent points under a time-reversal symmetry operation. Physically, this means that there is an energetic cost (charged to the system!) to go from **K** to **K**$'$. This would not happen if the points were equivalent.